

Doping Dependence of the Pseudogap in $\text{La}_{2-x}\text{Sr}_x\text{CuO}_4$

J. G. Naeini, X. K. Chen, and J. C. Irwin

Department of Physics, Simon Fraser University, Burnaby, British Columbia, V5A 1S6, Canada

M. Okuya,* T. Kimura,† and K. Kishio

Department of Superconductivity, University of Tokyo, Bunkyo-ku, Tokyo 113, Japan
(Phys. Rev. B59, 1 April 1999)

We report the results of Raman scattering experiments on single crystals of $\text{La}_{2-x}\text{Sr}_x\text{CuO}_4$ that span the range from underdoped ($x = 0.10$) to overdoped ($x = 0.22$). The spectra are consistent with the existence of a strong anisotropic quasiparticle interaction that results in a normal state depletion of spectral weight from regions of the Fermi surface located near the zone axes. The strength of the interaction decreases rapidly with increasing hole concentration and the spectral evidence for the pseudogap vanishes when the optimum doping level is reached. The results suggest that the pseudogap and superconducting gap arise from different mechanisms.

PACS numbers: 74.25.Gz, 74.72.Dn, 74.25-q, 78.30.Er

I. INTRODUCTION

It has been recognized for some time^{1,2} that the normal state electronic properties of the high temperature superconductors (HTS) are very different from those of a conventional Fermi liquid. It is also generally agreed that an understanding of the normal state properties is important in identifying the physical mechanism responsible for superconductivity in HTS. As a result an increasing amount of attention has focused on the temperature region $T > T_c$ and recent studies³⁻¹⁷ of underdoped compounds have revealed remarkable deviations from Fermi liquid behavior. These results⁴⁻¹⁷ have been interpreted in terms of the opening of a normal state pseudogap (PG), a term that is generally used to mean a large suppression of low energy spectral weight.

Despite an extensive experimental effort the physical origin of the PG remains undetermined. Some of the proposed mechanisms involve precursor pairing^{3,18,19} at $T > T_c$. For example Emery and Kivelson¹⁸ have suggested that incoherent pairs form above T_c , with phase coherence and hence superconductivity occurring at T_c . Or if one has separation of charge and spin¹⁹ d-wave pairing of spinons can take place at $T > T_c$, with charge condensation at T_c . On the other hand in the nearly antiferromagnetic Fermi liquid (NAFL) model proposed by Pines and coworkers²⁰⁻²², the PG and superconducting mechanisms are competing. In this model the PG or spectral weight depletion (SWD) is caused by strong anisotropic antiferromagnetic (AFM) interactions that are peaked near the AFM ordering vector $\mathbf{Q} = (\pi, \pi)$.

To obtain additional, complementary information on the nature and extent of the PG regime we have carried out electronic Raman scattering experiments on $\text{La}_{2-x}\text{Sr}_x\text{CuO}_4$ [$\text{La}_{214}(x)$]. This compound is an excellent material for these studies for several reasons. It has a relatively simple structure with a single CuO_2 plane in the primitive cell. Thus the results are not influenced by structural complications such as those introduced by the chains in $\text{YBa}_2\text{Cu}_3\text{O}_y$ (Y123) or the structural modula-

tions in $\text{Bi}_2\text{Sr}_2\text{CaCu}_2\text{O}_z$ (Bi2212). Finally the hole concentration is determined simply by the Sr concentration if oxygen stoichiometry is maintained. As a result, one can obtain²³ high quality and well characterized single crystals of La_{214} that enable one to study the systematic evolution of the electronic properties throughout the complete doping range. We have measured the relative strengths and frequency distributions of the B_{1g} and B_{2g} Raman continua as a function of temperature and doping. The results of these experiments are consistent with a PG mechanism that is intrinsic to a single CuO_2 layer and is present only in the underdoped regime of La_{214} . Our results also imply that the energy scale E_g associated with the PG is quite different from the superconducting gap energy Δ .

II. EXPERIMENT

The samples studied in this work were grown by a travelling floating-zone method²³. The crystals used here were cut from larger single crystals and typically had dimensions of about $2 \times 2 \times 0.5 \text{ mm}^3$. Characterization of the samples included susceptibility and transport measurements of their critical temperatures²³. The sample surfaces were prepared for light scattering experiments by polishing with diamond paste and etching²⁴ with a bromine-ethanol solution. Finally the samples were oriented in the basal plane using Laue x-ray diffraction patterns. The physical parameters characterizing the La_{214} samples are summarized in Table I.

The Raman spectra were obtained in a quasibackscattering geometry using the 488.0 or 514.5 nm lines of an Ar^+ laser. In most cases the light was focussed onto the sample using a cylindrical lens, but on occasion a combination of a spherical and cylindrical lenses was used to reduce the dimensions of the laser beam at the sample. In all cases the incident power level was controlled to be less than 10 W/cm^2 . With these power levels an estimate of about 11 K has been obtained for the amount of local

$\text{La}_{2-x}\text{Sr}_x\text{CuO}_4$	Nominal Sr content (x)	T_c ($^\circ\text{K}$)
Underdoped	0.10	27
Underdoped	0.13	35
Optimally doped	0.17	37
Overdoped	0.19	32
Overdoped	0.22	30

TABLE I. The physical parameters characterizing the samples studied in this paper. T_c was determined magnetically and x is the nominal hole concentration²³.

heating by the laser. This estimation was obtained from measurements of the power dependence of the spectra at temperatures near T_c , and the Stokes/anti-Stokes ratio at somewhat higher temperatures. The temperatures reported in this paper are the ambient value plus 11 K, or the estimated temperature in the excited region of the sample.

In a Raman spectrum the intensity of the scattered light is proportional to the square of the Raman tensor γ , whose components can be selected by appropriate choices of the incident and scattered polarizations²⁵. In this paper spectra were obtained in the $z(xy)\bar{z}$ and $z(x'y')\bar{z}$ scattering geometries where the letters inside the brackets denote the polarizations of the incident and scattered light. Here the x and y axes are parallel to the Cu-O bonds and x' and y' axes are rotated by 45° with respect to (x, y) . The xy component of the Raman tensor γ_{xy} transforms as $k_x k_y$ or the B_{2g} irreducible representation of the D_{4h} point group, and $\gamma_{x'y'}$ as $(k_x^2 - k_y^2)$ or B_{1g} . Thus $\gamma(B_{1g})$ must vanish along the diagonal directions $(\pm 1, \pm 1)$ in k -space and $\gamma(B_{2g})$ must vanish along the k_x and k_y axes. These two scattering geometries allow us to probe complementary regions of the FS²⁵ since the B_{1g} channel will sample regions of the FS located near the k_x and k_y axes while the B_{2g} channel will probe regions located near the diagonal directions.

Throughout this paper we deal with the frequency distribution of the Raman response function $\chi''(\omega, T)$ which is obtained by dividing the measured intensity by the thermal factor $[1 - \exp(-\hbar\omega/k_B T)]^{-1}$.

III. RESULTS

A detailed description of Raman spectra of La214(0.17) sample, which we will consider to be representative of the optimally doped state, has been published recently²⁵. In this paper we will focus on the changes that occur in the spectra of the underdoped and overdoped compounds. We will first discuss spectra obtained from the underdoped samples ($x = 0.10$ and 0.13). The normal state response functions are shown in Fig. 1 for the 0.13 sample and the low temperature response functions for both samples are presented in Fig. 2. As is shown in Fig. 1a, the magnitude of $\chi''(B_{1g})$ is independent of tempera-

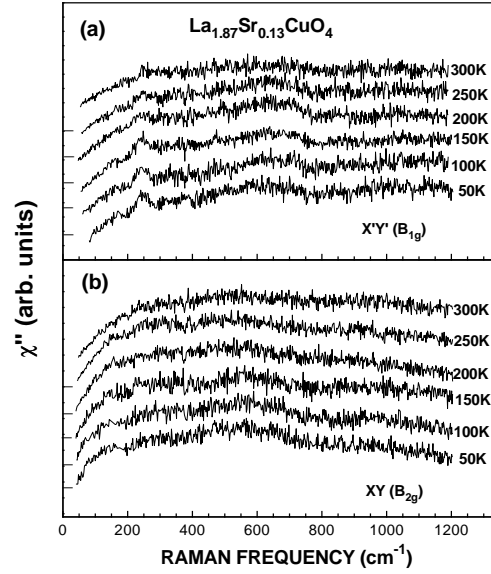


FIG. 1. The B_{1g} (a) and B_{2g} (b) response functions of the underdoped La214(0.13) crystal for temperatures between 50K and 300K. The spectra are offset vertically for clarity.

ture, to within the accuracy of our measurements (15%). From figures 2a and 2b, it is evident that the B_{1g} spectra obtained for each sample, above and below T_c , are essentially identical and are thus unaffected by the superconducting (SC) transition. In direct contrast, the low energy B_{2g} spectra of both underdoped compounds (Figs. 2c and 2d) undergo a superconductivity induced renormalization (SCIR) as the temperatures of the samples are lowered through T_c . The observed immunity of the B_{1g} spectra to passage into the SC state, and contrasting SCIR in the B_{2g} channel, is analogous to the behavior observed in underdoped Y123¹³.

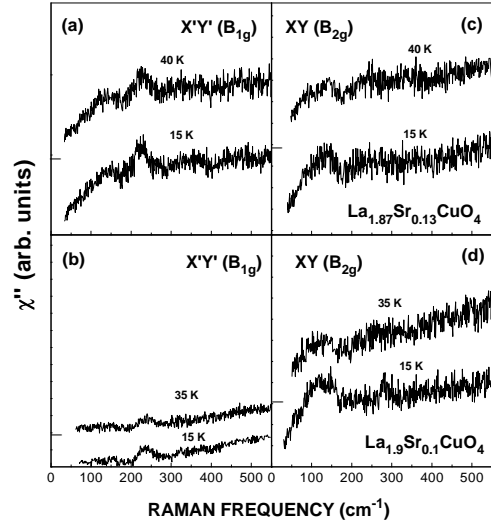


FIG. 2. The B_{1g} response above and below T_c for the La214(0.13) crystal (a) and the La214(0.10) crystal (b). The B_{2g} response for the same crystals are shown in (c) and (d).

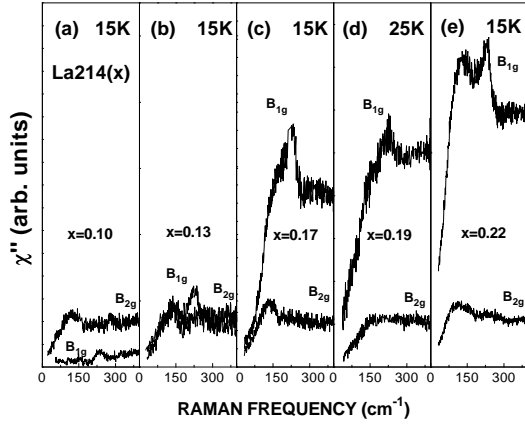


FIG. 3. Direct Comparison of the low energy B_{1g} and B_{2g} Raman response functions measured at temperatures below T_c in $\text{La}_{214}(x)$ for (a) $x = 0.10$; (b) $x = 0.13$; (c) $x = 0.17$; (d) $x = 0.19$; and (e) $x = 0.22$. The scale of χ'' is the same for all five frames.

We have also obtained spectra from two overdoped crystals ($x = 0.19$ and 0.22) and we have found that the magnitude of the response functions $\chi''(B_{1g})$ in both samples (for $\omega \geq 300 \text{ cm}^{-1}$) are again approximately independent^{26,27} of temperature. In contrast to the situation in the underdoped samples, there is a pronounced SCIR that occurs at T_c in *both* the B_{1g} and B_{2g} channels for both the optimally doped²⁵ and the overdoped samples^{26,27}. Finally the low temperature spectra of the overdoped crystals, in both B_{1g} and B_{2g} channels, are compared to the underdoped and optimally doped spectra in Fig. 3.

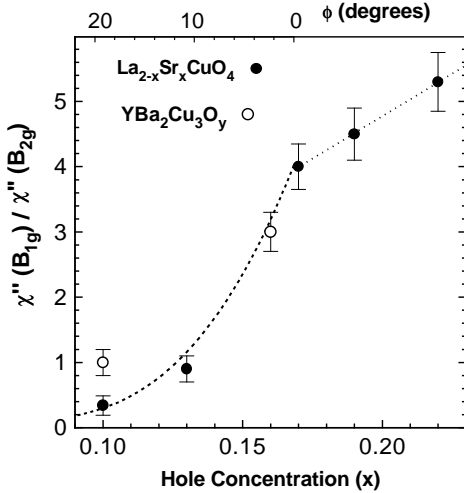


FIG. 4. The ratio R of the integrated Raman response functions plotted as a function of hole concentration for $\text{La}_{2-x}\text{Sr}_x\text{CuO}_4$ (●) and $\text{YBa}_2\text{Cu}_3\text{O}_y$ (○). The ratio was determined for $0 \leq \omega \leq 600 \text{ cm}^{-1}$ in all cases. The dashed line represents the calculated R using equation (1) for different values of ϕ (Fig. 5) superimposed using the top scale. The dotted line serves only as a guide to the eye.

As a measure of the strength of the response functions we will use the integral of $\chi''(\omega)$ over the low frequency spectral region. In this context the strength of $\chi''(B_{2g})$ is approximately the same (Fig. 3) for all the crystals studied here, while the strength of $\chi''(B_{1g})$ changes dramatically as we proceed from the underdoped to the overdoped samples. The ratio $R = \int d\omega \chi''(B_{1g}) / \int d\omega \chi''(B_{2g})$, and therefore the strength of the B_{1g} Raman response, increases by a factor of about 16 as we go from the underdoped $x = 0.10$ sample to the optimally doped sample with $x = 0.17$. The ratio R continues to increase, but at a slower rate as one proceeds into the overdoped regime. This result is summarized quantitatively in Fig. 4, where we have plotted the ratio R as a function of hole concentration. For comparison purposes, data obtained previously¹³ on Y123 are also included²⁸ in Fig 4. It is evident that the ratio R for the two compounds exhibits a similar trend with doping.

IV. DISCUSSION

A. Spectral Weight Depletion

Relatively few Raman experiments have been carried out to investigate the nature of the PG. Nemetschek *et al.*¹⁴ have attributed a small loss of spectral weight at $\omega \leq 700 \text{ cm}^{-1}$ in the B_{2g} channel to the presence of a PG. Blumberg *et al.*¹⁵, in spectra obtained from underdoped Bi2212 have observed a sharp feature at about 600 cm^{-1} which they have attributed to a bound state associated with precursor pair formation above T_c . In our studies of underdoped Y123 and La214 we have focused on the striking loss of spectral weight in the B_{1g} channel, and the contrasting constancy of the B_{2g} spectra, features which appear to be common^{13,29,30} to the hole doped cuprates.

To illustrate the dramatic change in the intensity in the B_{1g} channel and the relative constancy of the B_{2g} channel, we can calculate the unscreened Raman response functions in the superconducting state using the conventional model of light scattering³¹

$$\chi''_{\gamma}(\omega) \propto \left\langle \frac{\gamma^2(\mathbf{k})\Delta^2(\mathbf{k})}{\omega\sqrt{\omega^2 - 4\Delta^2(\mathbf{k})}} \right\rangle, \quad (1)$$

where $\langle \dots \rangle$ imply an average over the FS for \mathbf{k} -vectors such that $\omega > 2|\Delta(\mathbf{k})|$. The results shown in Fig. 5 were obtained with $\gamma(\mathbf{k})$ calculated using a second neighbor tight binding model with the parameters described previously²⁵ and $\Delta(\mathbf{k}) = \Delta_0[\cos(k_x a) - \cos(k_y a)]$. The response functions obtained by integrating (1) over the full FS (dashed lines in the inset of Fig. 5) are shown in Fig. 5a. To obtain a representation of the Raman response in the underdoped case we integrate (1) over portions of the FS lying between ϕ and $90^\circ - \phi$ in each quadrant. That is, regions of the FS near the axis (defined by angle ϕ) were excluded from the integration, and

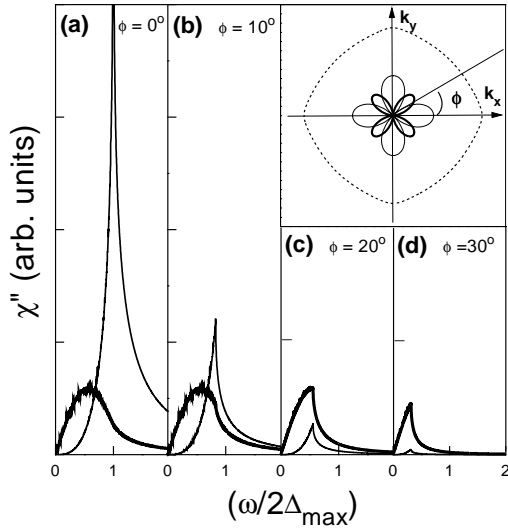


FIG. 5. Calculated B_{1g} (thin lines) and B_{2g} (thick lines) Raman response functions in La214 (a) by integrating over the full Fermi surface (dashed lines in the inset) and (b-d) by integrating only over region lying between ϕ and $90^\circ - \phi$ in each quadrant. The inset shows polar plots of the angular dependence of the B_{1g} (thin lines) and B_{2g} (thick lines) components of the Raman tensor $\gamma(\mathbf{k})$.

the resulting response functions are shown in Figs. 5b-5d for $\phi = 10^\circ$, 20° , and 30° . As is evident an increasing truncation of the FS leads to a rapid depletion of the B_{1g} spectrum, but has much smaller effect on the B_{2g} spectrum.

We have also calculated the ratio R of the integrated response functions as a function of ϕ and the results are superimposed (dashed line) on the data points in Fig. 4. For the purpose of this comparison both the measured and calculated response functions were integrated from $\omega = 0$ to 600 cm^{-1} . It should be noted that the apparent agreement between calculation and experiment is quite fortuitous given the simplistic nature of the model. The results do, however, provide plausibility to the existence of localized depletion of spectral weight from regions of the FS located near $(\pi, 0)$. Finally we should note that the effective gapping of quasiparticles (QP) from these same region, at $T > T_c$, is consistent with the absence of a superconductivity induced renormalization in the B_{1g} spectra of the underdoped compounds (Figs. 2a and 2b).

The observed dependence on scattering geometry thus implies that the spectral weight loss is confined to regions of the FS located near $(\pm\pi, 0)$ and $(0, \pm\pi)$ and that QP located near the diagonals are essentially unaffected by a reduction in doping level. Given that ARPES experiments⁸⁻¹⁰ also find a SWD that reaches a maximum in regions near $(\pi, 0)$, we will assume that this feature is characteristic of the PG, and that the PG thus manifests itself in the Raman spectra *primarily* as a SWD in the B_{1g} channel. We should note however, that the B_{2g} spectra is also approximately independent of tem-

perature (for $T > T_c$), which is difficult to reconcile with the FS contraction envisaged by Norman *et al.*¹¹.

According to Fig. 4 the SWD or pseudogap has approximately the same strength in La214 and Y123. This is not consistent with the suggestion³² that the PG arises from strong AFM interactions between the closely spaced CuO_2 layers of bilayer compounds such as Y123. The present results thus suggest that the PG arises from intralayer interactions and in this regard are in agreement with IR^{4,5}, ARPES⁷, specific heat³³, and NMR³⁴ measurements.

B. Magnitude (E_g) of the Pseudogap

In the spectra we have obtained from La214 there is no clear indication of an onset temperature T^* for the PG. Estimates^{21,34} of $T^* \leq 200 \text{ K}$ have been obtained from the analysis of NMR experiments carried out on slightly underdoped La214 samples ($x = 0.14$ and 0.15). On the other hand transport³⁵, IR reflectivity⁵, and specific heat³³ measurements on underdoped La214 have all found $T^* > 300 \text{ K}$. Our spectra (Fig. 1) indicate some minor changes at about 200 K , that include the appearance of a broad and weak feature at about 600 cm^{-1} in both channels. In fact the variations that occur in the B_{2g} spectra below about 200 K reflect a decrease in intensity at low energies similar to that observed by Nemetschek *et al.*¹⁴ in Bi2212. However, no significant changes in spectral weight, which one might expect to mark the onset of the PG, occur at any temperature below 300 K .

The lack of an experimental consensus for T^* in La214 is perhaps supportive of the suggestion³⁶ that one cannot associate a well defined T^* with the PG, but only an energy scale E_g . In this regard, however, there is also no clear evidence of a gap edge in the B_{1g} spectra we have obtained (Fig. 1) from underdoped La214. This is perhaps not surprising if E_g is of order of J in underdoped samples and decreases with increasing hole concentration as has been suggested by photoemission⁷ and specific heat³³ measurements. This magnitude for the PG might be expected if short range AFM correlation were responsible for the spectral weight depletion²⁰. One possible scenario involves the existence of AFM ordered regions and separate hole rich regions in the underdoped samples. Evidence for this type of phase separation was obtained recently in the muon spin resonance experiments on underdoped La214 and Ca doped Y123³⁷.

In Raman spectra one-magnon excitations are not observed and hence the PG energy would be reflected in the two-magnon peak that occurs at about $3J \approx 3000 \text{ cm}^{-1}$ in undoped La214^{38,39} and insulating Y123^{38,40,41}. The amplitude and energy of the two-magnon peak decreases^{39,42} as the compounds are doped and such peaks have not been observed for doping levels greater than or equal to optimum. Although our spectrometer range is limited, we have carried out preliminary measurements of the

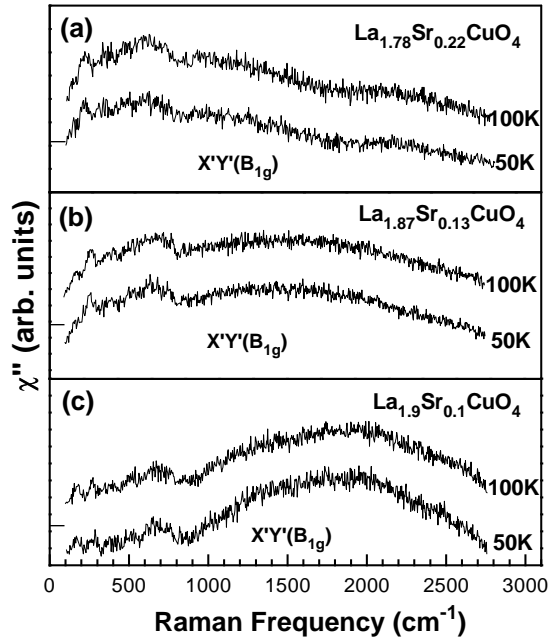


FIG. 6. The high energy B_{1g} Raman response functions measured at 50 K and 100 K in $\text{La}_{214}(x)$ for (a) $x = 0.22$, (b) $x = 0.13$, and (c) $x = 0.10$.

high energy B_{1g} spectra for three samples ($x = 0.10, 0.13$, and 0.22). The high energy ($\omega < 3000 \text{ cm}^{-1}$) response functions measured at 50 K and 100 K for the three samples are shown in Fig. 6. From the figure one can see a broad, weak peak at about 2000 cm^{-1} ($J \sim 700 \text{ cm}^{-1}$) in the $x = 0.10$ spectrum. This peak essentially vanishes as we proceed to higher doping levels (Figs. 6a and 6b). We must emphasize that these spectra have not been corrected for variations in the optical constants or for spectrometer response and are shown only to illustrate the effect of doping. Our spectrometer response decreases in the red and correction might push the peak in Fig. 6c to higher energies and also decrease its relative amplitude. Such corrections would not however alter the observed trend that is induced by changes in doping.

It appears plausible that the pseudogap or SWD in the B_{1g} channel is due to short range AFM correlations and the formation of “hot spots”²⁰ on regions of the FS located near $(\pm\pi, 0)$ and $(0, \pm\pi)$. As the doping level is increased the AFM interactions become weaker, as is evidenced by a weakening (Fig. 6) and shift of the two-magnon peak to lower energies^{39,42}. Thus as the doping level is increased, E_g decreases and some spectral weight is shifted from higher to lower energies. At optimum doping, where a SCIR is observed in the B_{1g} channel (Fig. 3c), the PG is assumed to be filled. Furthermore on the basis of their specific heat measurements in several cuprates Loram *et al.*³³ have proposed that $E_g \approx J(1 - p/p_{cr})$ where p is the hole concentration and p_{cr} the value at which E_g “closes”. Given that $J \approx 1000 \text{ cm}^{-1}$ in La_2CuO_4 and $E_g \approx 700 \text{ cm}^{-1}$ (Fig.

6c) suggests $p_{cr} > p_{opt}$. We would thus conclude that the pseudogap “fills” before it “closes”.

It is interesting to compare the PG energy scale E_g to that of the superconducting gap Δ . In Raman spectra the energy of the pair-breaking peak in the B_{1g} channel can be used⁴³ as a measure of Δ . In optimally doped La_{214} the maximum value of the superconducting gap²⁵ is given by $\omega(B_{1g}) \approx 2\Delta_{max} \approx 200 \text{ cm}^{-1}$, as is also evident from Fig. 3. In the overdoped region Δ_{max} decreases (Fig. 3), consistent with the behavior in other cuprates^{44–46}. In the underdoped regime the absence of SCIR in the B_{1g} channel means that we do not have any direct measure of the gap maxima. We can note however that the frequency of the pair-breaking peak in the B_{2g} channel remains approximately constant [$\omega(B_{2g}) \approx 130 \pm 20 \text{ cm}^{-1}$] as the doping level is decreased from optimum. We thus infer that Δ remains approximately constant throughout the doping range $0.10 \leq x \leq 0.17$. This behavior is also consistent with that found in ARPES and tunneling measurements^{9,47} on Bi_{2212} . Therefore we have an amplitude $\Delta_{max} \approx 100 \text{ cm}^{-1}$ for the SC gap and $E_g \sim J \sim 700 \text{ cm}^{-1}$ for the PG. These very different energy scales suggest that different physical mechanisms are involved.

C. Summary

The most noticeable aspect of the spectra shown in Fig. 3 is the SWD that occurs in the B_{1g} channel when the doping level is reduced below optimum, while the strength of the B_{2g} spectrum is essentially unaffected by changes in doping. These results suggest that the QP scattering rate is highly anisotropic⁴⁸ and leads to the existence of “hot spots” on regions of the FS located near $(\pm\pi, 0)$ and $(0, \pm\pi)$. This observation is consistent with the predictions of Pines and coworkers²⁰ who have pointed out that QP located near these regions can be coupled by the AFM ordering vector $\mathbf{Q} = (\pi, \pi)$ and hence interact strongly in underdoped compounds. Conversely, the QP on regions of the FS located near $|\mathbf{k}_x| = |\mathbf{k}_y|$ are weakly coupled²⁰, and have been designated as “cold”^{20,49}. As the doping level is increased toward optimum the SWD decreases rapidly, consistent with a weakening of the AFM interactions between QP²⁰. In this language our results then suggest that the hot QP are gapped above T_c and hence are not affected by the SC transition. Only the cold QP, as evidenced by the SCIR in the B_{2g} channel at T_c , participate in the transition to the SC state.

Thus far our attention has been focused on the most dominant feature of the spectra obtained from underdoped compounds, namely the SWD that is confined to the B_{1g} channel. As mentioned previously Nemetschek *et al.*¹⁴ found that a relatively small depletion of spectral weight also occurs in the B_{2g} channel of Y_{123} and Bi_{2212} below $\omega \approx 700 \text{ cm}^{-1}$ and $T \approx 250 \text{ K}$. This en-

ergy and onset temperature are in good agreement with IR measurements on the same compounds⁴. This appears reasonable since, given the SWD in the B_{1g} channel one would expect the results of IR and transport measurements, for example, to be determined mainly by the properties of the cold QP^{14,20,49}, or those on regions of the FS located near the diagonal directions. Furthermore, one can see that a similar small depression of spectral weight appears below 700 cm⁻¹ and 200 K in the B_{2g} spectra of the x = 0.13 crystal (Fig. 1b), in agreement with IR measurements carried out⁵ on underdoped La214. Thus the loss of spectral weight in the B_{2g} channel¹⁴, the depression of the scattering rate observed in IR experiments, and the spectral weight depletion observed in the B_{1g} channel (Figs. 3 and 4) are all characterized by the same energy scale. This suggests that there is a common physical mechanism underlying the apparently different phenomena that are observed in the two channels. However, the identification of a possible interrelation between the two channels will require a very careful analysis of temperature dependence of the spectra for 50 K ≤ T ≤ 300 K. Such an analysis should also provide important information about the existence and magnitude of crossover temperatures T* that have been observed in other experiments^{5,21,34,35} and are important features of some models^{18,20}. It is also possible that the SWD in the two channels arises from different mechanisms and that there are different pseudogaps as have been suggested⁷ by Ino *et al.*

V. CONCLUSIONS

In the Raman spectra obtained from La214 there is a loss of low energy spectral weight in the B_{1g} channel as the doping level is decreased below optimum, while the intensity in the B_{2g} channel remains unchanged. These results imply the existence of a strong anisotropic scattering mechanism and the formation of hot spots²⁰ on regions of the Fermi surface located near k_x and k_y axes. Furthermore, in underdoped compounds the B_{1g} channel is unaffected by the superconducting transition. The pseudogap is thus manifested in Raman spectra both by a depletion of low energy spectral weight or reduced intensity and by the absence of a superconductivity induced renormalization in the B_{1g} channel. In this context the pseudogap in La214 and Y123¹³ is present only in the underdoped regime. Since the spectral weight depletion is similar in the two compounds, we conclude that the pseudogap is intrinsic to a single CuO₂ plane and does not arise from interlayer interactions. Furthermore the results suggest that the loss of low energy intensity in the B_{1g} channel is due to strong antiferromagnetic interactions which in turn implies E_g ≈ J ≈ 700 cm⁻¹ for the pseudogap, an energy scale that is much larger than the energy of the superconducting gap (Δ_{max} ≈ 100 cm⁻¹). These energy scales imply that the pseudogap and super-

conducting gap arise from different physical mechanisms. Since superconductivity grows while the spectral weight loss or pseudogap diminishes, it appears that the two mechanisms compete with each other for the available quasiparticles.

VI. ACKNOWLEDGEMENTS

The authors gratefully acknowledge useful conversations with T. P. Devereaux, T. Startseva, T. Timusk, and J. Schmalian. One of us (JCI) has also benefited greatly from discussions with R. G. Buckley, J. L. Tallon, A. J. Trodhal, and G. V. M. Williams during a visit to the Industrial Research Laboratory in Lower Hutt, New Zealand. The financial support of the Natural Sciences and Engineering Research Council of Canada is gratefully acknowledged.

-
- ¹ P. B. Allen, Z. Fisk, and A. Miglieri, *Physical Properties of HTS*, V. I, edited by D. M. Ginsberg (World Scientific, Singapore, 1989).
 - ² I. Bozovic, D. Kirillov, A. Kapitulnik, K. Char, M. R. Hahnan, M. R. Beasley, T. H. Geballe, Y. H. Kim, A. J. Heeger, *Phys. Rev. Lett.* **59**, 2219 (1987).
 - ³ M. Randeria, in *Proc. of Internat. School of Phys.*, Verenna, 1997, edited by G. Iadonisi and J. R. Schrieffer (IOS Press, Amsterdam, 1998); cond-mat/9710223.
 - ⁴ A. V. Puchkov, D. N. Basov, and T. Timusk, *J. Phys. Condensed. Matter* **8**, 10049 (1996); A. V. Puchkov, P. Fournier, T. Timusk, and N. N. Kolesnikov, *Phys. Rev. Lett.* **77**, 1853 (1996).
 - ⁵ T. Startseva, T. Timusk, A. V. Puchkov, D. N. Basov, H. A. Mook, T. Kimura, and K. Kishio, *Phys. Rev. B* **59** March 1 (1999); T. Timusk and B. Statt to be published in *Reports Progress in Physics*.
 - ⁶ C. P. Slichter, R. L. Corey, N. J. Curro, S. M. DeSoto, K. O'Hara, T. Imai, A. M. Kini, H. H. Wang, U. Geiser, J. M. Williams, K. Yoshimura, M. Katoh, and K. Kosuge, *Philosophical Magazine B* **74**, 545-561 (1996).
 - ⁷ A. Fujimori, A. Ino, T. Mizokawa, C. Kim, Z.-X. Shen, T. Sasagawa, T. Kimura, K. Kishio, M. Takaba, K. Tamasaku, H. Eisaki, and S. Uchida, *J. Phys. Chem. of Solids* **59**, 1892 (1998); A. Ino, T. Mizokawa, K. Kobayashi, A. Fujimori, T. Sasagawa, T. Kimura, K. Kishio, K. Tamasaku, H. Eisaki, and S. Uchida, *Phys. Rev. Lett.* **79**, 2101 (1997); *Phys. Rev. Lett.* **81**, 2124 (1998).
 - ⁸ D. S. Marshall, A.G. Loeser, Z.-X. Shen and D. S. Dessau, *Phys. Rev. Lett.* **76**, 4841 (1996); A. G. Loeser, Z.-X. Shen and D. S. Dessau, *Science* **273**, 325 (1996).
 - ⁹ J. M. Harris, Z.-X. Shen, P. J. White, D. S. Marshall, M. C. Schabel, J. N. Eckstein, and I. Bozovic, *Phys. Rev. B* **54**, R15 665 (1996).
 - ¹⁰ H. Ding, T. Yokoya, J. C. Campuzano, T. Takahashi, M.

- Randeria, M. R. Norman, T. Mochiku, K. Kadowaki, and J. Giapintzakis, *Nature* **382**, 51 (1996); H. Ding, M. R. Norman, T. Yokoya, T. Takeuchi, M. Randeria, J. C. Campuzano, T. Takahashi, T. Mochiku, and K. Kadowaki, *Phys. Rev. Lett.* **78**, 2628 (1997).
- ¹¹ M. R. Norman, H. Ding, M. Randeria, J. C. Campuzano, T. Yokoya, T. Takeuchi, T. Takahashi, T. Mochiku, and K. Kadowaki, P. Guptasarma, and D. G. Hinks, *Nature* **392**, 157 (1998).
- ¹² J. W. Loram, K. A. Mirza, J. R. Cooper, N. Athanasopoulou, and W. Y. Liang, P341 in *Proc. of 10th Anniversary HTS Workshop*, (World Scientific, Singapore, 1996).
- ¹³ X. K. Chen, J. G. Naeini, K. C. Hewitt, J. C. Irwin, R. Liang, and W. N. Hardy, *Phys. Rev. B* **56**, R513 (1997).
- ¹⁴ R. Nemetschek, M. Opel, C. Hoffmann, P. F. Muller, R. Hackl, H. Berger, L. Forro, A. Erb, and E. Walker, *Phys. Rev. Lett.* **78**, 4837 (1997).
- ¹⁵ G. Blumberg, M. Kang, M. V. Klein, K. Kadowaki, and C. Kendziora, *Science* **278**, 1427 (1997).
- ¹⁶ J. W. Quilty, H. J. Trodhal, and D. M. Pooke, *Phys. Rev. B* **57**, R11097 (1998).
- ¹⁷ J. L. Tallon, G. V. M. Williams, N. E. Flower, and C. Bernard, *Physica C* **282-287**, 236 (1997).
- ¹⁸ V. J. Emery and S. A. Kivelson, *Nature* **374**, 434 (1995); V. J. Emery and S. A. Kivelson, and O. Zachar, *Phys. Rev. B* **56**, 6120 (1997).
- ¹⁹ P. W. Anderson, *Science* **235**, 1196 (1987); X. G. Wen and P. A. Lee, *Phys. Rev. Lett.* **76**, 503 (1996).
- ²⁰ D. Pines, *Z. Phys. B* **103**, 129 (1997); *Physica C* **282-287**, 273 (1997).
- ²¹ V. Barzykin and D. Pines, *Phys. Rev. B* **52**, 13585 (1995); Y. Zha, V. Barzykin and D. Pines, *Phys. Rev. B* **54**, 7561 (1996).
- ²² A. V. Chubukov, D. Pines, and B. Stojkovic, *J. Phys.: Cond. Matter* **8**, 10017 (1996); J. Schmalian, D. Pines, and B. Stojkovic, *Phys. Rev. Lett.* **80**, 3839, (1998).
- ²³ T. Kimura, K. Kishio, T. Kobayashi, Y. Nakayama, M. Motohira, K. Kitazawa, and K. Yamafuji, *Physica C* **192**, 247 (1992).
- ²⁴ D. J. Werder, C. H. Chen, M. Gurvitch, B. Miller, L. F. Schneemeyer, and J. V. Waszczak, *Physica C* **160**, 411 (1989).
- ²⁵ X. K. Chen, J. C. Irwin, H. J. Trodhal, T. Kimura, and K. Kishio, *Phys. Rev. Lett.* **73**, 3290 (1994); *Physica C* **295**, 80 (1998).
- ²⁶ J. G. Naeini, X. K. Chen, K. C. Hewitt, J. C. Irwin, T. P. Devereaux, M. Okuya, T. Kimura, and K. Kishio, *Phys. Rev. B* **57**, R11077 (1998).
- ²⁷ J. G. Naeini, J. C. Irwin, M. Okuya, T. Kimura, T. Sasagawa, Y. Togawa, and K. Kishio, to be published.
- ²⁸ See J. L. Tallon, C. Bernard, H. Shaked, R. L. Hitterman, and J. D. Jorgensen, *Phys. Rev. B* **51**, 12911 (1995), for an estimation of the hole concentration in *Y123*.
- ²⁹ T. Katsufuji, Y. Tokura, T. Ido, and S. Uchida, *Phys. Rev. B* **48**, 16131 (1993).
- ³⁰ M. Opel, R. Nemetschek, C. Hoffmann, P. F. Muller, R. Philipp, R. Hackl, H. Berger, L. Forro, A. Erb, and E. Walker, *J. Phys. Chem. of Solids* **59**, 1942 (1998).
- ³¹ M. V. Klein and S. B. Dierker, *Phys. Rev. B* **29**, 4976 (1984).
- ³² A. J. Millis and H. Monien, *Phys. Rev. Lett.* **70**, 2810 (1993).
- ³³ J. W. Loram, K. A. Mirza, J. R. Cooper, *J. Phys. Chem. of Solids* **59**, 2091 (1998).
- ³⁴ H. Yasuoka, *Physica C* **282-287**, 119 (1997).
- ³⁵ B. Batlogg, H. Y. Hwang, H. Takagi, R. J. Cava, H. L. Kao, and J. Kwo, *Physica C* **235-240**, 130 (1994).
- ³⁶ G. V. M. Williams, J. L. Tallon, E. M. Haines, R. Michalak, and R. Dupree, *Phys. Rev. Lett.* **78**, 721 (1997).
- ³⁷ Ch. Niedermayer, C. Bernhard, T. Blasius, A. Golnik, A. Moodenbaugh, and J. I. Budnick, *Phys. Rev. Lett.* **80**, 3843 (1998).
- ³⁸ K. B. Lyons, P. A. Fleury, L. F. Schneemeyer, and J. V. Waszczak, *Phys. Rev. Lett.* **60**, 372 (1988); K. B. Lyons, P. A. Fleury, A. S. Cooper, and T. J. Negran, *Phys. Rev. B* **37**, 2353 (1988).
- ³⁹ S. Sugai, S. Shamoto, and M. Sato, *Phys. Rev. B* **38**, 6436 (1988).
- ⁴⁰ D. Reznik, S. L. Cooper, M. V. Klein, W. C. Lee, D. M. Ginsberg, A. A. Maksimov, A. V. Puchkov, I. I. Tartakovskii, S. Cheong, *Phys. Rev. B* **48**, 7624 (1993).
- ⁴¹ G. Blumberg, P. Abbamonte, M. V. Klein, W. C. Lee, D. M. Ginsberg, L. L. Miller, A. Zibold, *Phys. Rev. B* **53**, R11930 (1996).
- ⁴² M. Rubhausen, C. T. Rieck, N. Dieckmann, K. O. Subke, A. Bock, and U. Market, *Phys. Rev. B* **56**, 14797 (1997).
- ⁴³ T. P. Devereaux, D. Einzel, B. Stadlober, R. Hackl, D. H. Leach, and J. J. Neumeier, *Phys. Rev. Lett.* **72**, 396 (1994).
- ⁴⁴ X. K. Chen, E. Altendorf, J. C. Irwin, R. Liang, and W. N. Hardy, *Phys. Rev. B* **48**, 10530 (1994); X. K. Chen, J. C. Irwin, R. Liang, and W. N. Hardy, *J. Supercond.* **7**, 435 (1994); *Physica C* **227**, 113 (1994).
- ⁴⁵ P. J. White, Z.-X. Shen, J. M. Harris, A. G. Loeser, P. Fournier, A. Kapitulnik, *Phys. Rev. B* **54**, R15669 (1996).
- ⁴⁶ C. Kendziora, R. J. Kelley, and M. Onellion, *Phys. Rev. Lett.* **77**, 727 (1996).
- ⁴⁷ Ch. Renner, B. Revaz, J. -Y. Genoud, K. Kadowaki, and O. Fischer, *Phys. Rev. Lett.* **80**, 149 (1998).
- ⁴⁸ T. P. Devereaux and A. Kampf, *J. Phys. Chem. of Solids* **59**, 1972 (1998); (cond-mat/9711039).
- ⁴⁹ L. B. Ioffe and A. J. Millis, *Phys. Rev. B* **58**, 11631 (1998).

*Present address: Department of Material Science, Shizuoka University, Johoku, Hamamatsu 432, Japan.

†Present address: Joint Research Center for Atom Technology, Higashi, Tsukuba 305, Japan.